Int. J. Environ. Sci. Technol. (2014) 11:1035–1042
DOI 10.1007/s13762-013-0287-z

ORIGINAL PAPER

Caspian Sea level prediction using satellite altimetry by artificial neural networks

M. Imani · R.-J. You · C.-Y. Kuo

Received: 8 January 2013 / Revised: 4 March 2013 / Accepted: 17 March 2013 / Published online: 17 April 2013

Abstract The demand for accurate predictions of sea level fluctuations in coastal management and ship navigation activities is increasing. To meet such demand, accessible high-quality data and proper modeling process are critically required. This study focuses on developing and validating a neural methodology applicable to the short-term forecast of the Caspian Sea level. The input and output data sets used contain two time series obtained from Topex/Poseidon and Jason-1 satellite altimetry missions from 1993 to 2008. The forecast is performed by multilayer perceptron network, radial basis function, and generalized regression neural networks. Several tests of different artificial neural network (ANN) architectures and learning algorithms are carried out as alternative methods to the conventional models to assess their applicability for estimating Caspian Sea level anomalies. The results derived from the ANN are compared with observed sea level values and with the forecasts calculated by a routine autoregressive moving average (ARMA) model. Different ANNs satisfactorily provide reliable results for the short-term prediction of Caspian Sea level anomalies. The root mean square errors of the differences between observations and predictions from artificial intelligence approaches can be significantly reduced by about 50 % compared with ARMA techniques.

Keywords Artificial neural network · Sea level forecast · Caspian Sea · Satellite altimetry

M. Imani (✉) · R.-J. You · C.-Y. Kuo
Department of Geomatics, National Cheng Kung University, No. 1 University Road, Tainan 701, Taiwan
e-mail: p68997010@mail.ncku.edu.tw

Introduction

The measurements, analysis, and prediction of sea level fluctuations are considerably important for marine meteorology and operational oceanography, as these aspects could be successfully applied in coastal zone management (Cazenave et al. 2002; Pashova 2002).

Sea level variations are complex outcomes of various environmental factors, such as precipitation, runoff from neighbor catchments, evaporation, air and water temperature, water salinity, as well as the interaction between water body and low-lying aquifers. Contributions to sea level variations may vary from region to region. In addition, accurate measurements and analysis by conventional methods considering different effective contributions are still difficult to achieve and may have large uncertainties (Talebizadeh and Moridnejad 2011).

Instead of using models or environmental factors as inputs, some researchers have used historical sea level records to predict sea level variations. The most conventional technique for sea level prediction is based on the extrapolation of linear trends; however, irregular changes, such as the El Nino/Southern Oscillation, cannot be fully fitted. Irvine and Eberhardt (1992) developed multiplicative seasonal autoregressive integrated moving average (ARIMA) models for lakes Erie and Ontario using standardized monthly mean level data to predict up to 6 months of sea level. Sen et al. (2000) applied simple linear and periodic nonlinear models in modeling the deterministic part of lake level time series and a second-order Markov model in modeling the remaining stochastic part. However, traditional methods, such as the ARIMA or Box–Jenkins (Box et al. 1991), assume that a given time series is generated from an underlying linear process. Therefore, these methods may not always perform well when applied in modeling hydrological time series that are often nonlinear.

One of the useful computational techniques for sea level analysis and forecast is the artificial neural network (ANN). ANNs have become increasingly popular because of their independency with regard to the assumptions of functional models, the probability distribution, or the smoothness (Demuth et al. 2008). ANNs can approximately fit nonlinear mathematical functions and allow plausible simulations of the behavior of complex systems without any preceding knowledge of the internal relations among their components (Haykin 1999a).

Röske (1997) first applied ANNs to improve the forecast of the sea level along the German North Sea coast. Similarly, Vaziri (1997) used ANNs and ARIMA models to predict the monthly Caspian Sea level using tide gauge records at Anzali Port in Iran for the period of January 1986–December 1993.

The prediction of Caspian Sea level change by traditional methods is less accurate because of the nonlinear dynamic process of sea level data (Imani et al. 2012). Hence, the objective of the current study is to develop and validate a neural methodology applicable to short-term Caspian Sea level forecasts. We use 15-year Topex/Poseidon (T/P) and Jason-1 (J-1) altimetry data covering 1993–2008. The data were selected because of the highly accurate measurements and the optimal spatial locations of the ground tracks in the Caspian Sea compared with the tide gauge records conventionally used for predicting sea level variations. The following models are developed to forecast Caspian Sea level variations: (a) multilayer perceptron network (MLP); (b) radial basis function (RBF); (c) generalized regression neural networks (GRNNs); and (d) the autoregressive moving average (ARMA) technique.

The main goals of this study are as follows: (1) to test different ANN architectures and analyze their performances, as well as (2) to compare the outcomes with those derived from the conventional ARMA technique. An adequate ANN structure and a better model performance for each case are found using statistical indicators. Two altimetric data sets covering the period of 1993–2008 are used to train and test the neural networks.

Study area and data

The Caspian Sea, with a surface area of 371,000 km^2, is the largest inland water body on earth, with virtually no tides and a salinity of 13 mg/l. The present sea surface of the landlocked Caspian basin at approximately 27 m below global sea surface fluctuates rapidly on several time scales, from seasons to centuries. These fluctuations result from the interactions among river discharge (predominantly the Volga River), evaporation, precipitation, and water temperature (Rodionov 1994; Kostianoy and Kosarev 2005).

Measurements of Caspian Sea level variations covering the whole basin provide helpful information about the water mass balance as well as the interannual and decadal oscillations in response to climate changes. Sea level gauge records conventionally used for sea level monitoring are considerably affected by geographical and meteorological phenomena, including vertical crustal movements, changes in atmospheric pressure, wind, river discharge, water circulation, water density, and ice melting (Cazenave et al. 1997; Lebedev and Kostianoy 2008; Cretaux et al. 2011). However, the trends of vertical movements and sea level changes cannot be clearly distinguished when sea level gauges are used.

In the last two decades, satellite-based sensors, particularly satellite altimetry, have offered a promising alternative for monitoring water surfaces with an unprecedented high precision, from interseasonal to interannual time scales and covering regardless of meteorological and geological constraints (Cretaux et al. 2011; Lebedev and Kostianoy 2008).

As T/P and J-1 satellite altimeters can assess water surfaces with high accuracy and comprehensively cover the Caspian Sea with repeat ground tracks of 9.918 days, sea surface measurements from both altimeters covering the period of April 1993–January 2008 are employed in the present study to predict Caspian Sea level anomalies.

T/P altimeter data in the form of sea surface heights (SSHs) are extracted from the merged geophysical data record (GDR) provided by NASA Physical Oceanography Distributed Active Archive Center (PODAAC) at the Jet Propulsion Laboratory of the California Institute of Technology (Benada 1997). Similarly, SSHs of J-1 are retrieved from the interim GDR and the GDR provided by Archivage, Validation et Interprétation des données des Satellites Océanographiques and PODAAC (Picot et al. 2006).

Ground tracks of passes 092, 031, 016, 209, 133, and 057 are used in the study. Passes 168 and 224 are not used because of less accurate altimetric measurements resulting from strong winds, presence of ice, and shallow water (Fig. 1).

After the application of recommended corrections, including standard instrumental, media, and geophysical corrections, sea level anomalies (h_{SLA}) are calculated by subtracting from the corrected SSHs the geoid heights from the EGM2008 geopotential model (Pavlis et al. 2008). The time series of the along-track averaged Caspian Sea level anomalies for each repeat cycle covering 1993–2008 used in the study can be computed by

$$\overline{h_{\mathrm{SLA}}}(t) = \frac{1}{n}\sum_{1}^{n} h_{\mathrm{SLA}}(t,n) \tag{1}$$

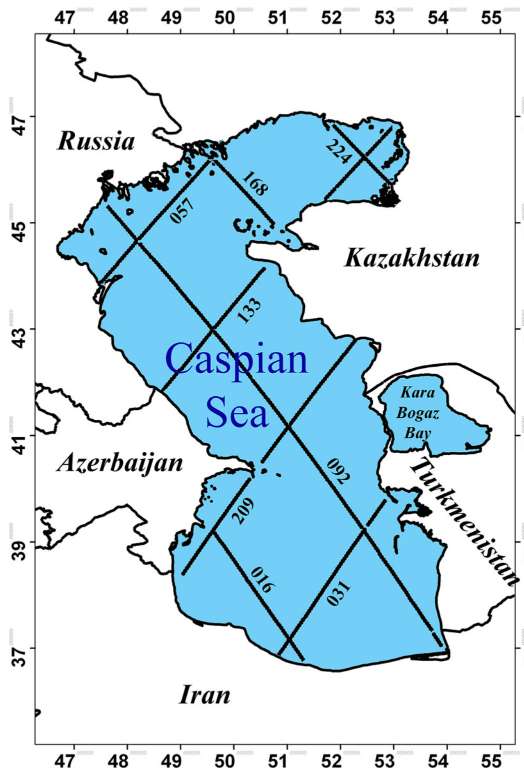

Fig. 1 T/P and J-1 ground tracks over the Caspian sea

where t is the index of cycles, and n is number of altimetric along-track measurements.

Materials and methods

Several neural network architectures can be applied for the forecast of water level fluctuations, which is a nonlinear dynamic process. ANN structures are massively distributed in parallel, thereby introducing a new computational technology that resembles the human information-processing system (Palit and Popovik 2005).

The neural networks are organized hierarchically by layers of neurons to process nonlinear signals. The information is collected in the input layer and is then forwarded to the network through processing by the hidden layer(s). This procedure continues down throughout the layers to the output layer, which presents the network results. The ANN computational process is divided into two stages: training and testing. During the training stage, the network is iteratively trained, and the interconnection weights and the biases between neurons are adjusted in each step so that the output value fits the desired input values. During the second testing stage, the network can be verified to make predictions using the data subset not presented in the training stage (Hagan et al. 1995). In the study, three multilayer structures of ANNs, namely, MLP, RBF, and GRNN, are developed.

Multilayer perceptron network

The MLP is a feedforward ANN model that associates sets of input data with a set of appropriate output. The MLP networks are an extension of perceptron networks containing one or more hidden layers. Each neuron computes a weighted sum of input signals by including a threshold value passing through the transfer function that generates the neuron output. The back propagation algorithm involving two phases is usually used for tainting MLP networks. During the first phase or the feedforward phase, the free network parameters do not change, and the input information is propagated through the network layer by layer. At the end of this phase, the network error value, which represents the difference between the desired response and the output produced by the network in response to the presented input vector, is computed. During the second phase or the backward phase, the free network parameters (weights and biases) are adjusted to minimize the network error, which is computed according to the error measurements (Cybenko 1989; Hornik et al. 1989).

MLPs are made up of neurons that contain information-processing features essential to its operation. The inputs, x_j, are related to the neuron by the synaptic weight, w_j. Mathematically, a neuron can be described as follows:

$$v_i = \sum_{j=0}^{p} w_{ij} x_j \tag{2}$$

$$y_i = \varphi(v_i - \theta_i) \tag{3}$$

where x_j ($j = 0,\ldots, p$) are the inputs, w_j ($j = 0,\ldots, p$) are the synaptic weights linking the input j from the neuron i, v_i is the weighted sum of inputs to neuron i, φ is the activation or transfer function, θ_i is the threshold value, and y_i is the output of the neuron i (Haykin 1999b).

Different MLP networks with one and two hidden layers are applied in this study. Logistic sigmoid as the transfer function in the hidden layer, linear transfer function in the output layer, and training (gradient descent back propagation) algorithm for network training are used for forecasting sea level changes.

Radial basis function (RBF)

The RBF network is a feedforward neural network that consists of three layers, namely, the input, hidden, and output layers. In RBF networks, the outputs are determined by computing the distance between the network inputs and the center of the hidden layer. Each neuron in the hidden layer has a parameter vector called the center and computes its output using an RBF. An output layer computes the linear weighted sum of the hidden neuron outputs and represents the response of the network (Cichocki and Unbehauen 1993).

A general expression of the network representing the output–input relation can be given as (Robert and Howlett 2001)

$$y_i = \sum_{j=1}^{M} \beta_j \phi_j(x) \tag{4}$$

where y_i is the network output, M is the number of hidden neurons, x is the input data, β_j is the output layer weights of the RBF network, and ϕ (x) is the Gaussian RBF given by

$$\phi_j(x) = \exp\left(-\frac{\| x - c_j \|^2}{\sigma_j^2}\right) \tag{5}$$

where C_j and σ_j are the center and width of jth hidden neuron, respectively, and ||.|| denotes the Euclidean distance.

General regression neural network (GRNN)

The GRNN model is a kind of radial basis network that is often used for regression problems (Cichocki and Unbehauen 1993). The GRNN structure comprises four layers: the input, pattern, summation, and output layers (Specht 1991).

The total number of observation parameters is equal to the number of input units in the input layer. The first layer is entirely associated to the second pattern layer. Each neuron in this layer presents a training pattern, and its output is a measure of the distance of the input from the stored patterns. The pattern layer is connected to the summation layer. Each pattern layer unit is connected to the two neurons in the summation layer, namely, the S-summation neuron and the D-summation neuron. The S-summation neuron calculates the sum of the weighted responses of the pattern layer, whereas the D-summation neuron is used to compute the unweighted outputs of the pattern neurons. The connection weight between the ith neuron in the pattern layer and the S-summation neuron is y_i, which represents the output value corresponding to the ith input pattern. In the case of the D-summation neuron, the connection weight is unity. The output layer merely divides the output of each S-summation neuron by that of each D-summation neuron, resulting in the predicted value of an unknown input vector x and in stored patterns x_i as (Specht 1991; Heimes and Heuveln 1998)

$$\hat{y}_i(x) = \frac{\sum_{i=1}^{n} y_i \exp\left[-D(x, x_i)\right]}{\sum_{i=1}^{n} \exp\left[-D(x, x_i)\right]} \tag{6}$$

where n indicates the number of training patterns. The Gaussian D function is defined as

$$D(x, x_i) = \sum_{j=1}^{p} \left(\frac{x_j - x_{ij}}{\zeta}\right)^2 \tag{7}$$

where p is the element number of an input vector. x_j and x_{ij} are the jth element of x and x_i, respectively, ζ is the so-called spread factor, the optimal value of which is often determined empirically (Kim et al. 2003). The function approximation is smoother in the large spread than in the small spread. However, using a very large spread requires a large number of neurons to fit a fast-changing function. Meanwhile, many neurons are required to fit a smooth function. The network may not be generalized well using a spread that is too small (Specht 1991). In this study, we analyze the effect of different spreads to determine the best one that achieves a minimum root mean square error (RMSE) for our problem.

Analysis of the result

In this study, the performance of the neural networks is evaluated using statistical evaluation criteria, including the correlation coefficient (R) and RMSE. The following formulas are used:

$$R = \left[\frac{\sum_{i=1}^{n}\left(y_i^0 - \overline{y^0}\right)\left(y_i^e - \overline{y^e}\right)}{\sqrt{\sum_{i=1}^{n}\left(y_i^0 - \overline{y^0}\right)\sum_{i=1}^{n}\left(y_i^e - \overline{y^e}\right)}}\right] \tag{8}$$

$$\mathrm{RMSE} = \sqrt{\frac{\sum_{i=1}^{n}\left(y_i^0 - y_i^e\right)^2}{n}} \tag{9}$$

where y_i^0 is the observed level, y_i^e is the estimated level, and n is the number of forecast level; $\overline{y^0}$ and $\overline{y^e}$ are the averages of observed and estimated levels, respectively.

Results and discussion

The Caspian Sea level anomalies observed by T/P and J-1 satellite altimeters were computed in this study according to Eq. (1). Table 1 represents the statistical characteristics of the data on Caspian Sea level covering the period of 1993–2008. Figure 2 illustrates the Caspian Sea level anomalies from pass 092 with a maximum value of −26.77 m in late spring of 1995 and a minimum of −27.81 m in late 2001, indicating significantly seasonal signals.

In ANN models, the selection of appropriate input variables is critical for a successful modeling. Some researchers (Sudheer et al. 2002; Aqil et al. 2007; Bilgili et al. 2007) have demonstrated the computation of statistical analysis, such as correlation as well as cross-, auto-, and partial auto-correlation, to determine the appropriate input variables.

In the present study, the predicted sea level anomalies of pass 092 were presented because the latter is a better indicator of Caspian Sea level anomalies. Pass 092 was selected because it holds more data and is relatively free of strong winds and ice. Herein, the sea level anomalies of passes 031, 016, 209, 133, and 057 ground tracks were used as the input layer of the network because they are highly correlated with those of pass 092 as an output layer (Table 2).

For ANN processing, sea level anomalies from altimeters covering 1993–2008 were divided into two parts. The first part covering the period of 1993–2004 was used for the training procedure, whereas the second part covering 2005–2008 was utilized for the testing procedure.

Table 1 Statistical characteristics of altimetry sea level anomalies in different ground tracks

Ground track	Min (m)	Max (m)	Number of records
Pass 092	−27.81	−26.77	531
Pass 016	−27.81	−26.73	531
Pass 031	−27.41	−26.41	531
Pass 057	−28.01	−26.73	531
Pass 133	−27.91	−26.96	531
Pass 209	−28.27	−27.32	531

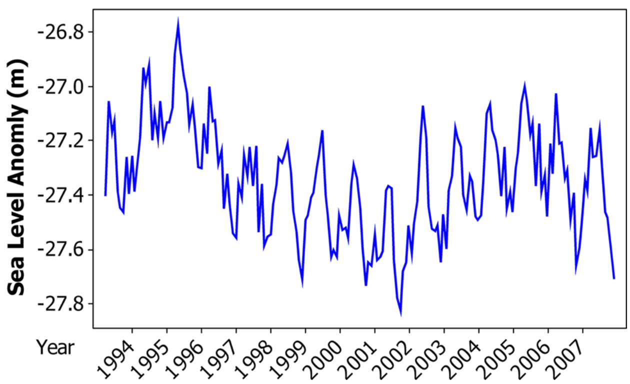

Fig. 2 Caspian Sea level anomalies of pass 092 from 1993 to 2008

Table 2 Correlation coefficients of sea level anomalies between pass 092 and other passes

Ground track	Pass 016	Pass 031	Pass 057	Pass 133	Pass 209
Correlation	0.91	0.81	0.77	0.88	0.83
P value*	<0.001	<0.001	<0.001	<0.001	<0.001

* *P* values <0.05 are considered statistically significant

We attempted to determine the appropriate model structure for the neural network applied in MLP, RBF, and GRNN architectures. Following routine procedures for the selection of the best ANN suited to the sea level data, different activation function options and network architectures were compared based on the work of Cichocki and Unbehauen (1993) and Demuth et al. (2008). Several trainings were performed to determine the number of hidden layers and the number of neurons in the hidden layers that provide the best testing performance for the aforementioned networks. The number of neurons in the hidden layer was chosen based on multiple reruns of different ANN structures with one or two hidden layers.

For the MLP architecture, MLP (x, y, z), x denotes the number of neurons in the input layer, y denotes the number of neurons in the hidden layers, and z denotes the number of neurons in the output layer. The optimal number of neurons in the hidden layer(s) was determined via the test simulation calculations using the statistical criteria (R and RMSE) between the observed and fitted (or predicted) data sets. Various combinations of different epochs and the number of neurons in the hidden layer(s) were tested using the MLP algorithm. A comparison is shown in Table 3.

As shown in Table 3, RMSE is reduced when two hidden layers are used instead of one hidden layer. The network structure, that is, MLP (5, 16–8, 1), with two hidden layers having 16 and 8 neurons and an input layer having 5 neurons and operated with 42 epochs provides the best performance. This network structure has the lowest centimeter-level RMSE and the highest R compared with the observed sea level values for the training and testing periods. However, MLP simulations have several drawbacks. After each simulation, different forecast values are obtained within the same network design because of the assignment of different initial random weights at the beginning of each training. To overcome this problem, simulations, even with the same network structure, were conducted several times until the best performance was

Table 3 RMSE and *R* for training and testing data sets using different MLP networks

Model	Training				Testing	
	No. of neurons in hidden layer	No. of epoch	RMSE (m)	*R*	RMSE (m)	*R*
MLP (5,4,1)	4	10	0.065	0.90	0.086	0.85
MLP (5,6,1)	6	50	0.045	0.92	0.061	0.90
MLP (5,8,1)	8	36	0.084	0.86	0.107	0.80
MLP (5,10,1)	10	100	0.106	0.82	0.124	0.78
MLP (5,6–3,1)	6–3	15	0.074	0.88	0.085	0.85
MLP (5, 16–6,1)	12–6	60	0.057	0.91	0.063	0.90
MLP (5,8–4,1)	8–4	110	0.097	0.83	0.111	0.79
MLP (5,16–8,1)	16–8	42	0.039	0.93	0.054	0.91
MLP (5,16–8,1)	16–8	42	0.042	0.93	0.060	0.91

obtained. The last two network structures in Table 3 are an example of this situation. The results of the estimations for the training and testing periods of the best MLP (5, 16–8, 1) compared with the observed sea level values are illustrated in Fig. 3. For the training period, the RMSE of the estimated and observed sea level anomalies were 0.039 m with an R of 0.93 and well-fitted seasonal and interannual signals. For the testing period, the RMSE was 0.054 m with a high R of 0.91, indicating that the model works excellently for sea level forecasting.

Different numbers of hidden layer neurons and spread constants were examined for the RBF and GRNN network

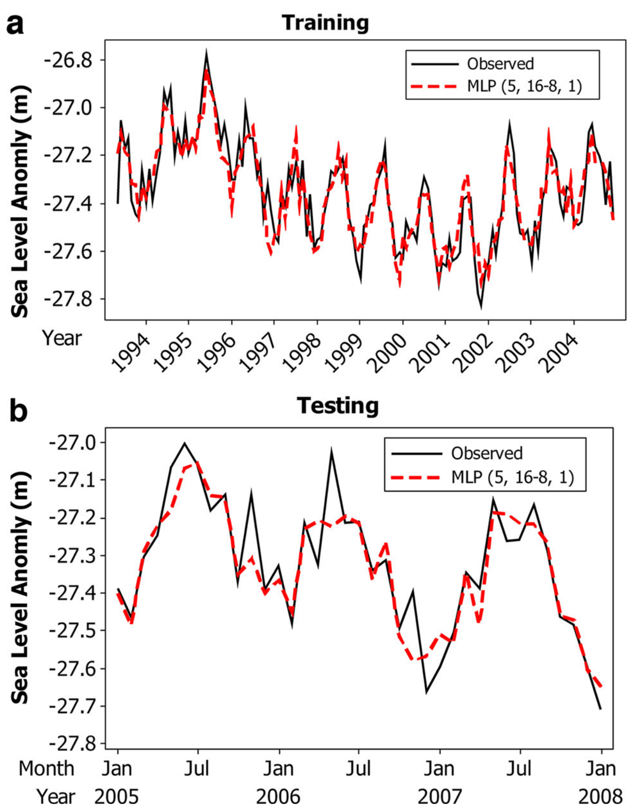

Fig. 3 Observed and estimated sea level anomalies of optimal MLP model during the **a** training and **b** testing periods

models (Table 4).The optimal RBF model was found to be the one that gave the minimum RMSE of 0.042 m and the highest R of 0.92 for the testing period with a spread constant of 0.45 and 22 neurons in the hidden layer. The estimations obtained from the RBF (5, 22, 1) network agree well with the observed sea level data (Fig. 4). Generally, the RBF model has better performance than the MLP. The most important advantage of the RBF model compared with the MLPs is its capability of obtaining the same forecast values for the same network architecture.

For the GRNN model, the network architecture of GRNN (5, 0.3, 1) with a spread parameter of 0.3 offered the best performance with the lowest RMSE of 0.059 m and the highest R of 0.90 for the testing period, as shown in Table 4 and Fig. 5.

To demonstrate the capability of the model to predict Caspian Sea level anomalies, a comparison was also made between the artificial network approaches and the convenient ARMA model, which is a traditional model based on the probability theory and statistical analysis. The model consists of two parts, namely, an autoregressive (AR) and a moving average (MA). This model is thus usually referred to as the ARMA (p, q) model, where p is the order of the AR, and q is the order of the MA (Box et al. 1991). Table 5 provides the error statistics of estimates using ARMA models during the testing period. The ARMA (3,3) model provides the optimal result for Caspian Sea level prediction (Fig. 6).

The statistics of the optimal model of neural networks and the ARMA models for validation are presented in Table 6. The RBF (5, 22, 1) networks with a spread constant of 0.45 were found to have the best performance, given the minimum RMSE and the maximum R during the training and testing periods. The ARMA model cannot surpass the ANNs in Caspian Sea level prediction, whereas the MLP, RBF, and GRNN models have similar accuracies. The RMSE obtained from the ANN method is reduced by about 50 %, and R increases more than 15 % compared with the values obtained from the ARMA method. This difference can be attributed to the fact that the ARMA model belongs to the

Table 4 RMSE and R for training and testing data sets using different RBF and GRNN networks

Model	Training				Testing	
	No. of neurons in hidden layer	Speed parameter	RMSE (m)	R	RMSE (m)	R
RBF (5, 11, 1)	11	0.50	0.087	0.85	0.095	0.82
RBF (5, 8,1)	8	0.55	0.055	0.91	0.063	0.90
RBF (5, 22, 1)	22	0.45	0.030	0.95	0.042	0.92
RBF (5, 33, 1)	33	0.65	0.065	0.90	0.083	0.85
GRNN (5,0.05,1)		0.05	0.087	0.85	0.102	0.80
GRNN (5, 0.5, 1)		0.50	0.069	0.89	0.091	0.83
GRNN (5, 0.3, 1)		0.30	0.047	0.92	0.059	0.90
GRNN (5, 0.1, 1)		0.10	0.098	0.83	0.127	0.78

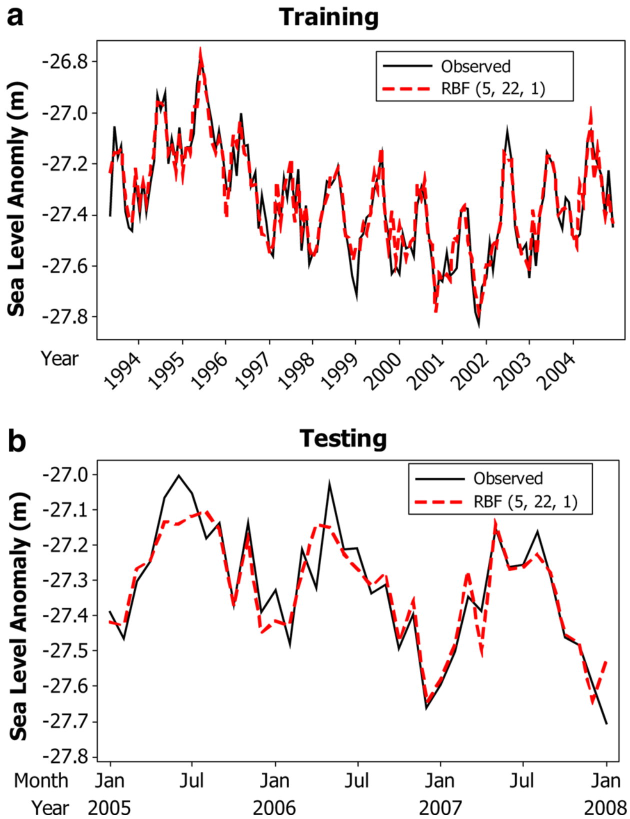

Fig. 4 Observed and estimated sea level anomalies derived by the optimal RBF model during **a** the training and **b** testing periods

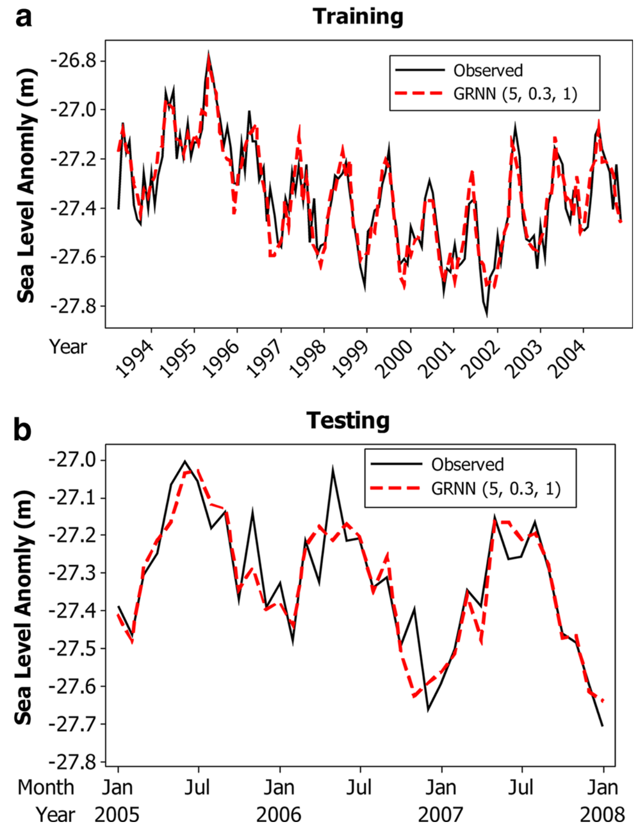

Fig. 5 Observed and estimated sea level anomalies derived by the optimal GRNN model during the **a** training and **b** testing periods

class of linear models that do not guarantee prediction accuracy, especially if the investigated phenomenon is nonlinear. The main advantages of ANN models are their flexibility and ability to model nonlinear relationships without any priori assumptions about the nature of the generating processes (ASCE Task Committee 2000). However, the ANN model requires a massive amount of data.

Conclusion

We applied approximately 15-year SSHs from T/P and J-1 satellite missions with highly accurate measurements and optimal spatial coverage over the Caspian Sea to predict the sea level in the area. Different ANN methods were employed to investigate the applicability of ANN algorithms in estimating Caspian Sea level anomalies and to examine the performance of each model.

The ANN method appeared as a powerful tool in predicting the Caspian Sea level depending on the correlation between the SSHs of different satellite ground tracks. The RBF method, as the best presented model in this study, has two advantages compared with others: saves computation time and provides the same forecast values while using the same network architecture.

Table 5 Testing statistics of estimates using ARMA models

Type of model	Statistics of ARMA models	
	RMSE (m)	*R*
AR (1)	0.138	0.76
AR (2)	0.137	0.76
AR (3)	0.126	0.78
ARMA (1,1)	0.127	0.78
ARMA (1,2)	0.123	0.78
ARMA (2,1)	0.125	0.78
ARMA (3,1)	0.121	0.78
ARMA (1,3)	0.125	0.78
ARMA (3,2)	0.121	0.78
ARMA (2,3)	0.121	0.78
ARMA (3,3)	0.119	0.79
ARMA (2,2)	0.121	0.78

We conclude that sea level anomalies can be predicted quickly and successfully without the use of any topographical details or other meteorological data as long as the required altimetric measurements are available. Using ANN models also provides significantly better and more precise predictions compared with the regression models.

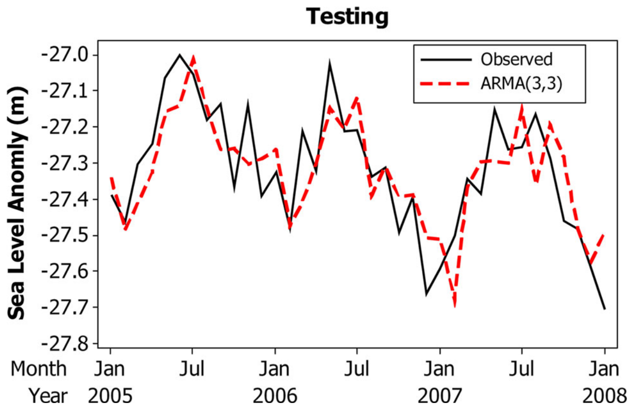

Fig. 6 Observed and estimated sea level anomalies derived by the optimal ARMA model during the testing period

Table 6 Error statistics of the optimal models during the testing period

Type of model	MLP (5,16–8,1)	RBF (5, 22, 1)	GRNN (5, 0.3, 1)	ARMA (3,3)
RMSE (m)	0.054	0.042	0.059	0.119
R	0.91	0.92	0.90	0.79

Acknowledgments This research is supported by the National Science Council of Taiwan (NSC 100-2221-E-006-234, NSC 101-2221-E-006-183). The co-author, Chung-Yen Kuo, is also partially supported by a grant from the National Science Council of Taiwan (NSC 101-2221-E-006-180-MY3). Altimeter data products are from AVISO (Archivage, Validation et Interprétation des données des Satellites Océanographiques). We thank anonymous reviewers and editor for their constructive comments.

References

Aqil M, Kita I, Yano A, Nishiyama S (2007) Analysis and prediction of flow from local source in a river basin using a neuro-fuzzy modeling tool. J Hydrol 85(1):215–223

ASCE Task Committee (2000) Artificial neural networks in hydrology I. J Hydrol Eng ASCE 5(2):115–123

Benada RJ (1997) Merged GDR (TOPEX/POSEIDON). Generation B users handbook, version 2.0, Physical Oceanography Distributed Active Archive Center (PODAAC), Jet Propulsion Laboratory, Pasadena, JPL D-11007, pp 131

Bilgili M, Sahin B, Yasar A (2007) Application of artificial neural networks for the wind speed prediction of target station using reference stations data. Renew Energ 32:2350–2360

Box GEP, Jenkins GM, Reinsel GC (1991) Time series analysis, forecasting and control. Prentice Hall, USA

Cazenave A, Bonnefond P, Dominh K, Schaeffer P (1997) Caspian Sea-level form Topex-Poseidon altimetry: level now falling. Geophys Res Lett 24:881–884

Cazenave A, Bonnefond P, Merciera F, Dominha K, Toumazou V (2002) Sea level variations in the Mediterranean Sea and Black Sea from satellite altimetry and tide gauges. Glob Planet Change 34(1–2):59–86

Cichocki A, Unbehauen R (1993) Neural networks for optimization and signal processing. Wiley, Chichester

Cretaux JF, Jelinski W, Calmant S et al (2011) SOLS: a lake database to monitor in the near real time water level and storage variations from remote sensing data. Adv Space Res 47:1497–1507

Cybenko G (1989) Approximation by superposition of a sigmoidal function. Math Control Signals Syst 2(4):303–314

Demuth HB, Beale MH, Hagan MT (2008) Neural network toolbox for use with MATLAB: user's guide, version 6. MathWorks, Inc., Natick

Hagan MT, Demuth H, Beale M (1995) Neural network design. PWS Publishing Company, Boston

Haykin S (1999a) Neural networks, a comprehensive foundation. Prentice Hall, Upper Saddle River

Haykin S (1999b) Neural networks: a comprehensive foundation. Prentice-Hall, Upper Saddle River, p 842

Heimes F, Heuveln B (1998) The normalized radial basis function neural network. Systems, man, and cybernetics. In Proceedings of the IEEE international conference on 11–14 October 1998 vol. 2, pp 1609–1614

Hornik K, Stinchcombe M, White H (1989) Multilayer feedforward networks are universal approximators. Neural Networks 2(5):359–366

Imani M, You RJ, Kuo CY (2012) Accurate forecasting of satellite-derived seasonal Caspian Sea level anomaly using polynomial interpolation and holt-winters exponential smoothing. Terr Atmospheric and Ocean Sci (in press)

Irvine KN, Eberhardt AJ (1992) Multiplicative, seasonal ARIMA models for Lake Erie and Lake Ontario water levels. Water Resour Bull 28(2):385–396

Kim B, Kim S, Kim K (2003) Modelling of plasma etching using a generalized regression neural network. Vacuum 71:497–503

Kostianoy AG, Kosarev AN (2005) The Caspian Sea environment. Springer, New York

Lebedev SA, Kostianoy AG (2008) Integrated use of satellite altimetry in the investigation of the meteorological. Hydrological, and hydrodynamic regime of the Caspian Sea. Terr Atmospheric Ocean Sci 19(1–2):71–82

Palit AK, Popovik D (2005) Advances in industrial control. In: Grimble MJ, Johnson MA (eds) Computational intelligence in time series forecasting: theory and engineering applications. Springer, London, pp 142–143

Pashova L (2002) Investigation of sea-level variations at two tide gauges in Bulgaria. In: Jozsef A, Schwarz KP (eds) Vistas for geodesy in the new Millennium, IAG symposia, vol 125. Springer, Berlin, pp 475–480

Pavlis N, Kenyon S, Factor J, Holmes S (2008) Earth gravitational model 2008. In SEG technical pro-gram expanded abstracts 27: 761–763

Picot N, Case K, Desai S, Vincent P (2006) AVISO and PODAAC user handbook. IGDR and GDR Jason products. SMM-MU-M5-OP-13184-CN (AVISO). JPL D-21352 (PODAAC). Edition 3, pp 112

Robert J, Howlett LCJ (2001) Radial basis function networks 2: new advances in design. Physica, Heidelberg. ISBN 3790813680

Rodionov SN (1994) Global and regional climate interpretation: the Caspian Sea experience. Kluwer Academic Publishers, Boston, p 241

Röske F (1997) Sea level forecasts using neural networks. Deutsche Hydrographische Zeitschrift 49(1):71–99

Sen Z, Kadioglu M, Batur E (2000) Stochastic modeling of Van Lake monthly level fluctuations in Turkey. Theoret Appl Climatol 65(1–2):99–110

Specht DF (1991) Enhancements to probabilistic neural network. In Proceedings of the international joint conference neural network 1: 761–768

Sudheer KP, Gosain AK, Ramasastri KS (2002) A data-driven algorithm for constructing artificial neural network rainfall–runoff models. Hydrol Process 16(6):1325–1330

Talebizadeh M, Moridnejad N (2011) Uncertainty analysis for the forecast of lake level fluctuations using ensembles of ANN and ANFIS models. Expert Syst Appl 38:4126–4135

Vaziri M (1997) Predicting Caspian Sea surface water level by ANN and ARIMA models. J Waterw Port Coast Ocean Eng 123:158–162